Materials Science & Engineering C 108 (2020) 110200

Contents lists available at ScienceDirect

Materials Science & Engineering C

journal homepage: www.elsevier.com/locate/msec

Fast, robust and effective decellularization of whole human livers using mild detergents and pressure controlled perfusion

Jorke Willemse, Monique M.A. Verstegen*, Annewiet Vermeulen, Ivo J. Schurink, Henk P. Roest, Luc J.W. van der Laan, Jeroen de Jonge

Department of Surgery, Erasmus MC-University Medical Center, Dr. Molewaterplein 40, 3015GD, Rotterdam, the Netherlands

ARTICLE INFO

Keywords:
Liver tissue engineering
Regenerative medicine
Whole organ decellularization
Extracellular matrix
Biomaterials
Liver transplantation

ABSTRACT

Human whole-liver perfusion-decellularization is an emerging technique for producing bio-scaffolds for tissue engineering purposes. The native liver extracellular matrix (ECM) provides a superior microenvironment for hepatic cells in terms of adhesion, survival and function. However, current decellularization protocols show a high degree of variation in duration. More robust and effective protocols are required, before human decellularized liver ECM can be considered for tissue engineering applications. The aim of this study is to apply pressure-controlled perfusion and test the efficacy of two different detergents in porcine and human livers.

To test this, porcine livers were decellularized using two different protocols; a triton-x-100 (Tx100)-only protocol (N = 3) and a protocol in which Tx100 was combined with SDS (N = 3) while maintaining constant pressure of 120 mm Hg. Human livers (N = 3) with different characteristics (age, weight and fat content) discarded for transplantation were decellularized using an adapted version of the Tx-100-only protocol. Decellularization efficacy was determined by histology and analysis of DNA and RNA content. Furthermore, the preservation of ECM components was assessed.

After completing the perfusion cycles with detergents the porcine livers from both protocols were completely white and transparent in color. After additional washing steps with water and DNase, the livers were completely decellularized, as no DNA or cell remnants could be detected. The Tx100-only protocol retained 1.5 times more collagen and 2.5 times more sGAG than the livers decellularized with Tx100 + SDS. The Tx100-only protocol was subsequently adapted for decellularizing whole-organ human livers. The human livers decellularized with pressure-controlled perfusion became off-white in color and semi-transparent within 20 h. Livers decellularized without pressure-controlled perfusion took 64–96 h to completely decellularize, but did not become white or transparent. The addition of pressure-controlled flow did remove all cells and double stranded DNA, but did not damage the ultra-structure of the ECM as was analyzed by histology and scanning electron microscopy. In addition, collagens and sGAG were maintained with the decellularized ECM.

In conclusion, we established effective, robust and fast decellularization protocols for both porcine and human livers. With this protocol the duration of decellularization for whole-organ human livers has been shortened considerably. The increased pressure and flow did not damage the ECM, as major ECM components remained intact.

1. Introduction

Liver decellularization procedures are attractive techniques for producing bio-active support scaffolds for liver tissue engineering purposes [1–3]. Currently, the only effective treatment for end-stage liver failure is liver transplantation [4]. However, an ever increasing gap exists between the high demand and the low availability of good quality donor livers, causing waitlist mortality [5,6]. The multidisciplinary field of liver tissue engineering aims to bridge this gap. Functional and transplantable liver constructs are created by combining supportive scaffold structures with functional cells and certain biochemical cues [3,7–9].

The scaffold, functional cells and biochemical cues are each of key importance for the functioning of the liver construct [3]. Researchers have put much effort in culturing primary hepatocytes *in vitro*. However, *in vitro* cultures lack the spatiotemporal control of physical and biochemical cues of the *in vivo* hepatic microenvironment. Therefore, these cells quickly dedifferentiate and loose functionality [10,11].

* Corresponding author.
E-mail address: m.verstegen@erasmusmc.nl (M.M.A. Verstegen).

https://doi.org/10.1016/j.msec.2019.110200
Received 14 June 2019; Received in revised form 21 August 2019; Accepted 11 September 2019
Available online 12 September 2019
0928-4931/

Similarly, the lack of these tissue specific cues is preventing the full differentiation of stem cells towards functional hepatocytes *in vitro* [12,13]. Therefore, a bio-mimicking support structure is required, which is capable of providing the hepatic cells with physical (e.g. stiffness and composition) and biochemical support (e.g. specific deposition of growth factors) [3,14–16].

In essence, the supportive scaffold has to replace the extracellular matrix (ECM) of the liver, which is composed of a complex mixture of extracellular matrix proteins (such as collagens, fibronectin and elastin), polysaccharides and proteoglycans (such as various glycosaminoglycans (GAGs)) [1,14,17,18]. Alterations in the composition and/or stiffness of the ECM can impair liver functionality and are associated to various disease states, such as liver fibrosis or cirrhosis [14,17,19]. Therefore, re-creating such a highly complex microenvironment which is capable of supporting cell proliferation and functionality is a challenging task. Instead of putting a lot of effort and resources in 're-inventing the liver ECM wheel', the use of native liver ECM as a basis for liver tissue engineering could be explored [16]. Poor quality donor livers, which are otherwise discarded for liver transplantation, are a useful source of liver ECM. Whole organ liver decellularization is a technique to remove all cellular material from the liver ECM, while retaining the liver architecture and all ECM components [16,20]. These structures are vital for the proper functioning of a tissue engineered liver construct [3].

Many studies showed the feasibility of liver decellularization of small animal livers, such as rodent livers [1,17,21–23]. However, efficient decellularization procedures for large-size livers, which potentially could be used in a clinical setting, are reported less frequently [15,24–27]. For human whole-organ liver decellularization, Mazza et al. showed (n = 1) feasibility of whole-organ human liver decellularization using perfusion with Triton-x-100 (Tx100) and sodium dodecyl sulfate (SDS) for 6 weeks [28]. We previously have shown procedures to decellularize whole human livers (n = 11) using only the milder detergent Tx100 to avoid damaging or removing ECM components [20]. The livers were completely decellularized (as confirmed by histology and DNA analysis). However, the time required per liver varied. The decellularization protocol used set flow rates, not taking in account the characteristics of the liver (e.g. size of the organ, age or level of steatosis). Larger sized livers might require higher flow rates for proper perfusion through the entire organ.

Recently, it has been shown that oscillating pressure conditions improved perfusion-based decellularization of both small animal (rat) [23] and large animal (porcine) livers [25]. Similarly, the addition of pressure controlled perfusion, where a constant pressure of 120 mm Hg is maintained, could make the decellularization of human livers quicker and more standardized, as flow through the organ might be improved, regardless of size of the liver.

In addition to improve perfusion through the liver, the use of detergents can also be further optimized. Many whole-organ liver decellularization protocols use a combination of Tx100 and SDS [1,15,21–25]. SDS is a harsh detergent, with a higher efficiency in removing the nucleus, when compared to Tx100. SDS is also known for inflicting damage to or removal of essential ECM components, such as GAGs [1,29]. Although we showed feasibility of Tx100-only whole organ liver decellularization in our series (N = 11) [20], we have not made a direct comparison between the two detergent protocols to assess this difference in efficacy of human whole-liver decellularization.

To improve whole-organ liver decellularization, we hypothesized that combining pressure controlled flow conditions using machine perfusion techniques and mild Tx100 as a detergent would yield a highly standardized human liver decellularization protocol for production of clinical grade bio-scaffolds, which retain more ECM components than with Tx100 plus SDS protocols. The first step in this study was to create a new decellularization setup with oscillating pressure conditions and compare the dual detergent protocol (Tx100 and SDS) to a Tx100-only protocol. After establishment of an optimal protocol in porcine livers, the optimal protocol was translated into a robust and reproducible protocol for whole human livers.

2. Material and methods

2.1. Porcine liver decellularization

Porcine livers (N = 6) were obtained from pigs ranging from 30 to 40 kg that were used for acute terminal medical research experiments (DEC 105-14-05) The use of the liver after termination was waived by the animal welfare committee of the Erasmus University Medical Center to comply with the 3R rule (replacement, reduction, refinement) in the use of lab animals. Animals were completely heparinized (300 IU/kg body weight) before they were euthanized. After retrieval of the liver it was cannulated via the hepatic artery and the portal vein. Subsequently, livers were flushed with 2 L of cold 0.9% NaCl solution prior to storage at −20 °C. Livers were subdivided into two groups. One group (n = 3) was decellularized using Tx100-only, the other group was decellularized using a combination of Tx100 and SDS (n = 3). Porcine livers were thawed overnight and small wedge-biopsies were taken from the peripheral edge of the organ to be analyzed as non-decellularized samples. One piece of biopsy tissue was fixated in 4% paraformaldehyde (PFA) overnight to be further processed for paraffin-embedding. Two other biopsies were snap-frozen and stored at −80 °C for further DNA, GAG or collagen content analysis. Biopsies were collected and processed at each biopsy/evaluation point.

The liver was placed in the decellularization setup, which is schematically represented in Fig. 1A. The cannulas were connected to peristaltic pump tubing (Hepatic artery: L/S #18 PharMed® BPT Tubing (Masterflex, Cole-Parmer), Portal vein: L/S #36 PharMed® BPT Tubing (Masterflex, Cole-Parmer)). The tubing was connected to a L/S® Precision pump peristaltic pump (Masterflex, Cole-Parmer) with two Easy-Load™ peristaltic pump heads (Masterflex, Cole-Parmer). The difference in diameter of both types of tubing created a difference in flow (1:1.26 according to manufacturer). The pump heads have 4 rollers each, which create a pulsatile flow with pressure differences. Pressure was measured using DTXplus Invasive blood pressure (IBP) transducers (BD). Perfusion was pressure-controlled with the upper limit for the hepatic artery pressure set at 120 mm Hg. RPM of the pump drive was adjusted accordingly.

The porcine livers were decellularized according to two different protocols: a Tx100-only protocol and a Tx100 + SDS protocol. Both protocols are schematically represented in Fig. 1B. The first step in both protocols was continuous perfusion with 20 L dH_2O. This was followed by continuous perfusion with 10 L of 4% Tx100 + 1% NH_3 (Tx100 solution). Subsequently, the livers from the Tx100-only group were perfused for 120 min with Tx100 solution. After 120 min the perfusate was replaced with fresh Tx100 solution and perfused for another 120 min. This was followed by three more cycles of 120 min (total number of cycles was 5). Group 2 was perfused for 120 min with 10 L Tx100 solution. After the 120 min cycle, the Tx100 solution was replaced with a 1%SDS solution and the liver was perfused for another 120 min. This was followed by 120 min perfusion with Tx100 and 120 min perfusion with SDS.

The livers were inverted every hour and stored overnight in 4 L dH_2O at 4 °C in between cycles if necessary. After completion of reperfusion cycles, livers from both groups were continuously perfused with 50 L dH_2O to remove residual detergents. Subsequently, the livers were stored in sealed containers filled with 10 L dH_2O for up to 10–14 days to passively remove any trace detergent. The water was refreshed every 1–2 days. In the last step, DNase solution (5 mg/L DNase type I (Sigma) in 0.9% NaCl + 100 mM $CaCl_2$ + 100 mM $MgCl_2$) was perfused through the liver for 120 min at 37 °C. Small biopsies were taken for detailed analysis.

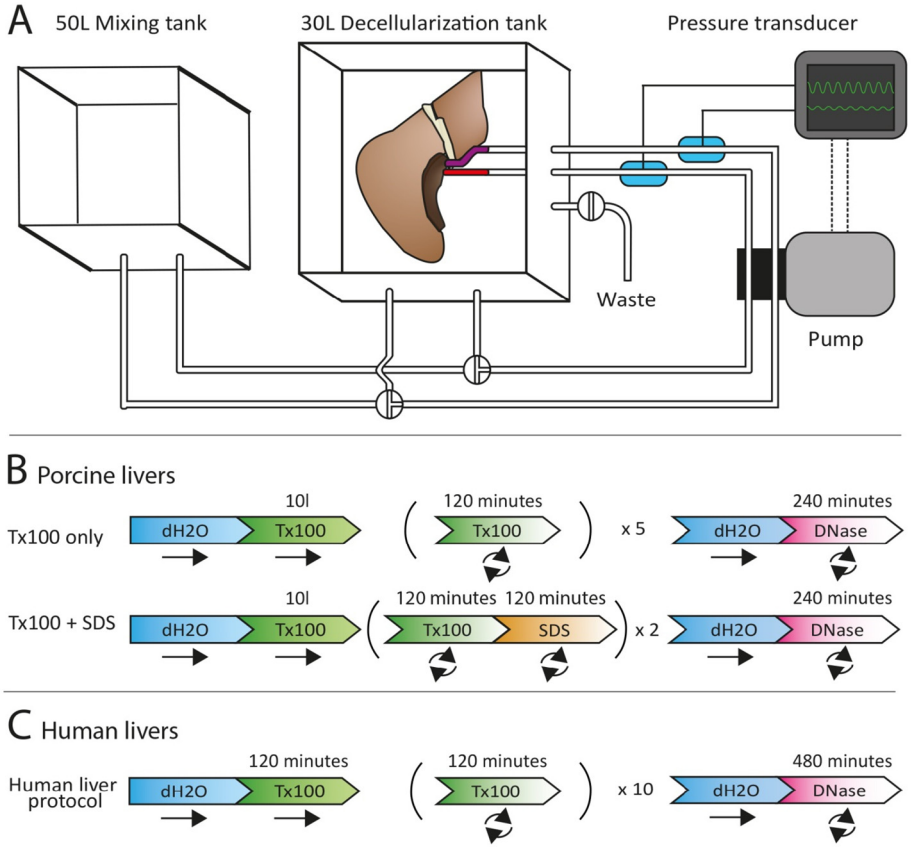

Fig. 1. A schematic overview of the decellularization setup and protocols used for porcine and human livers. A: the decellularization setup. The liver is placed in the decellularization tank and connected to the pump tubing via the hepatic artery and the portal vein. The pump tubing is connected to a pressure transducer, which relays pressure information to the dual headed pump drive. Three-way valves are used to create a closed loop for reperfusion or an open loop for continuous loop. A 50 L mixing tank is used to prepare detergents and/or fluids. The 50 L mixing tank can be exchanged. Waste is discarded via a manually operated valve. B: schematic representation of both porcine liver decellularization protocols. C: schematic representation of the human liver decellularization protocol. Total time required to complete decellularization was on average 14 h in group Tx100-only, 12 h in Tx100-SDS and 32 h in human whole livers (not including the 10–14 days storage period at 4 °C to passively remove traces of detergent.

2.2. Human liver decellularization

Human research livers were obtained after rejection for clinical liver transplant by all transplant centers in the Eurotransplant zone. Next of kin gave informed consent for research to Transplant Coordinators of the Dutch Transplant Foundation (NTS) present at the organ retrieval procedure. The use of research livers was approved by the Erasmus MC medical ethics committee (MEC-2012-090). Human livers with research consent (N = 3) were retrieved by organ retrieval teams during retrieval of other organs for transplantation. No organ retrieval was initiated for research purposes only. After organ retrieval according to the ET manual, chapter 5, livers were stored in UW on melting ice and shipped to the Erasmus MC. After cannulation of hepatic artery and portal vein, organs were stored at −20 °C until the decellularization procedure was started.

After the liver was thawed, it was placed in the decellularization setup (Fig. 1A). The procedure was similar to the procedure for porcine livers. Pressure on the hepatic artery was set at 120 mm Hg. Residual blood was removed from the organ by continuously perfusing with dH_2O until the perfusate changed from clear red to a turbid brown/orange solution (on average 50 L dH_2O was required). This was followed with 120 min of continuous perfusion with Tx100-only solution. Subsequently, the liver was perfused with a 10 L Tx100 solution for 10 times 120 min. The livers were inverted every hour.

In between cycles the liver could be stored at 4 °C in a sealed container filled with dH_2O overnight if necessary. Subsequently, the liver was perfused with 100 L dH_2O to remove residual detergents. The livers were stored in sealed containers filled with 10 L dH_2O for up to 10–14 days. The water was refreshed every 1–2 days. DNase solution (10 mg/L DNase type I (Sigma) in 0.9% NaCl + 100 mM $CaCl_2$ + 100 mM $MgCl_2$) was perfused through the liver for 8 h at 37 °C. Biopsies were taken afterwards.

2.3. Analysis

2.3.1. Histology

PFA-fixated biopsies were embedded in paraffin according to standard procedures and sectioned at 4 μm. Sections were stained with Hematoxylin-Eosin (HE), DAPI (Vectashield, Vectorlabs) or picrosirius red (PSR, Sigma) for overview, DNA remnants and collagens, respectively. In addition, Sudan B black staining was performed on paraffin sections to determine the presence of lipofuscin in the human livers. To detect fat residues in the decellularized livers, cryosections prepared from snap-frozen biopsies were stained with Oil red O.

HE, Sudan B black, PSR and Oil red O stained slides were imaged with a Zeiss Axiokop 20 microscope and captured with a Nikon DS-U1 camera. DAPI stained slides were analyzed using EVOS microscope (Thermofisher).

2.3.2. Scanning electron microscopy

PFA-fixated biopsies of human livers were dehydrated in a series of ethanol solutions (3 × 50%, 1 × 60%, 1 × 70%, 1 × 80% and 3 × 100%) for 15 min per step. This was followed by a dilution series with hexamethyldisilazane (Sigma) (1:2 HMDS: 100% ethanol, 2:1 HMDS: 100% ethanol and 3 times 100% HMDS). The samples were submerged in 1MHMDS and left uncovered inside a fume hood to air-dry overnight. HMDS treated samples were made electrically conductive with a 15 μm gold nanoparticle coating using a Quorum Q300T D sputtering device (Quorumtech). Samples were imaged using a JSM-7500F field emission electron microscope (JEOL).

2.3.3. DNA-RNA content

Prior to DNA or RNA isolation the wet weight of the biopsies was measured. DNA was isolated using a QIAamp DNA Mini Kit (QIAGEN) kit. DNA yield was measured using a NanoDrop spectrophotometer (Thermo Fisher Scientific). For the human livers, the DNA quality and

length of base pairs was measured using a 2100 BioAnalyzer (Agilent technologies) using a DNA-1000 kit (Agilent Technologies).

RNA from human livers was isolated using a miRNeasy Mini Kit (Qiagen). RNA yield was measured using a NanoDrop spectrophotometer (Thermo Fisher Scientific). For the human livers, the quality of RNA and the length of RNA base pairs were measured using a 2100 BioAnalyzer using a RNA 6000 Nano kit. The RNA concentration of the before samples (T = 0) was diluted five times with dH_2O before loading them on a chip.

2.3.4. GAG and collagen content

The sGAG content of snap frozen biopsies from both porcine and human livers was determined using the Blyscan™ Glycosaminoglycan Assay (Biocolor, UK) kit. The wet weight of biopsy samples was determined before they were digested at 65 °C with Papain (10 mg/ml, Sigma) for 8 h. SGAG was measured in the tissue digest according to the manufacturer's protocol. Absorbance was measured at 680 nm using a Model 680 XR Microplate Reader (Bio-Rad).

The total collagen content of snap frozen biopsies of both porcine and human livers was determined using a total collagen kit (Quickzyme biosciences). The wet weight of biopsy samples was determined before they were digested and measured according to manufacturer's protocol. Absorbance was measured at 570 nm using an Omega POLARstar Microplate reader (BMG labtech).

2.3.5. Immunohistochemistry of human livers

Collagen type I, III and IV were chosen because of their abundance in the liver ECM, their role in biological processes [19] and the potential role they could play in downstream liver tissue engineering purposes [3]. Immunohistochemistry (IHC) was performed on paraffin embedded sections of human livers from the experimental protocol. After deparaffinization, antigen retrieval was performed in a citrate buffer (pH = 6.0) at sub-boiling temperatures for 20 min. Collagen type I (1:100, Novus Biological), Collagen type III (1:100, Novus Biological) and Collagen type IV (1:100, Novus Biological) primary antibodies were added and incubated overnight at 4 °C. No primary antibody was added to negative control slides. Rabbit-*anti*-mouse or mouse-*anti*-rabbit secondary antibody (Envision Flex HRP, Agilent) were incubated for 60 min at RT prior to incubation with DAB substrate. Hematoxylin was used as a background staining. Slides were imaged with a bright field microscope.

2.4. Recellularization experiments

2.4.1. HEPG2 cells

HEPG2 cells were cultured in DMEM (Gibco) supplemented with 10% fetal calve serum (Sigma) and 1% (100U/ml) penicillin/streptomycin (PS) (Gibco). The HEPG2 were genetically labelled by transduction of a GFP-expression vector using a 3rd generation lentiviral vector according to standard procedure [30]. Gene expression efficiency was ~100%.

2.4.2. Two-dimensional recellularization experiments

Cylindrical plugs were punched from frozen human decellularized livers using a disposable dermal biopsy punch (Ø5mm). The plugs were embedded in optimal cutting temperature (OCT) compound (Tissue-Tek) and circular discs (200 μm thick) were cut using a cryotome (Leica). The discs were collected and washed in 1X PBS (5x times), 1X PBS + 1% PS (3x times) and 1xPBS + 10% PS (3x times). After the last washing step, the discs were incubated overnight in PBS + 10% PS. The discs were washed with 1X PBS and DMEM, before being placed in a 48-wells plate (Bio-Greiner).

HEPG2 cells were harvested using Trypsin-EDTA and counted. Per disc 10.000 cells were added in a droplet of 10 μl. The ECM discs plus cell suspension were incubated at 37 °C and 5% CO_2 for 4 h before 500 μl of cell culture medium was added. Samples were kept in culture for up to 21 days.

Samples were fixed in 4% PFA for 30 min for histological evaluation.

2.4.3. Three-dimensional perfusion recellularization experiments

Decellularized porcine livers (Tx100 only group) were segmented into smaller perfusable segments by tracing the artery. The segments roughly were 5–10 cm in length and width. The segments were cannulated with tubing from BD connecta 10 cm extension lines with 3-way stopcock.

The cannulated segments were perfused with 1x PBS (50 ml), 1x PBS + 1% PS (50 ml) and 1x PBS + 10% PS (50 ml). The segment was incubated over night at 37 °C with in 50 ml 1X PBS + 10% PS. Afterwards, the segment was washed with DMEM. The segment was placed inside a humidified chamber and connected to an isolated liver perfusion setup (Harvard Apparatus) via the 3-way stopcock. The perfusion setup was kept at 37 °C and pH, pO_2 and pCO_2 were monitored. O_2 and CO_2 were mixed and adjusted to maintain pH = 7.4. Once connected, the segments were constantly perfused with DMEM at a rate of 5 ml/min. HEPG2 were harvested and counted. 300 million cells were injected via the 3-way stopcock in 10 stages every 10 min under constant perfusion. The segments were incubated inside the humidified chamber at 37 °C. Experiments lasted 5 days (N = 1), 8 days (N = 1) and 11 days (N = 1).

At the end of each experiment, the segment was taken out of the perfusion setup and imaged using an EVOS microscope, before the segments were fixed in 4% PFA overnight for histological evaluation.

2.5. Statistical analysis

Analysis of numerical data was performed with Prism (version 5.0, Graphpad Software). Data from DNA, RNA, total collagen content, sGAG content and the nano indentations is displayed as mean + standard deviation (SD). One-way ANOVA (post-hoc Bonferroni) was used to analyze means.

3. Results

3.1. Porcine liver decellularization

Residual blood was washed out and the perfusate turned from a clear red solution to a more orange/brownish solution. The livers became pink in color (Fig. 2A). Moments after the start of pressurized perfusion with Tx100, small gray spots appeared near the surface of the liver demonstrating removal of cells and cellular debris. The bulk of the liver became white during the first 30–60 min of perfusion. Small pink areas were seen near peripheral edges of some, but not all, liver segments (Supplementary Video 1). These pink areas became white and transparent before the end of the perfusion cycles. During the first 30–60 min of perfusion with detergent, RPM of the pump drive had to be increased to an average of 125RPM (SD: 20RPM) to maintain constant perfusion pressure to 120 mm Hg. After the first hour only minor adjustments (± 5 RPM) were required to maintain hepatic artery pressure. Portal vein pressure differed per liver ranging from 20 mm Hg to 60 mm Hg.

Supplementary video related to this article can be found at https://doi.org/10.1016/j.msec.2019.110200.

The perfusion times with detergent for both protocols were (10 h (Tx100-only) and 8 h (Tx100 + SDS). Total perfusion times (including wash steps with dH_2O and DNase) were 14 and 12 h respectively. No macroscopic differences were seen (Fig. 2A and B) between the livers from the Tx100-only group and Tx100 + SDS group. The livers were white and transparent around the edges. In the center the light path was obscured by denser honeycomb-like white structures (Supplementary Fig. 1A). Microscopic analysis (HE Fig. 2 DEF, DAPI Fig. 2 GHI) did not reveal any differences between the two protocols. All cell remnants and

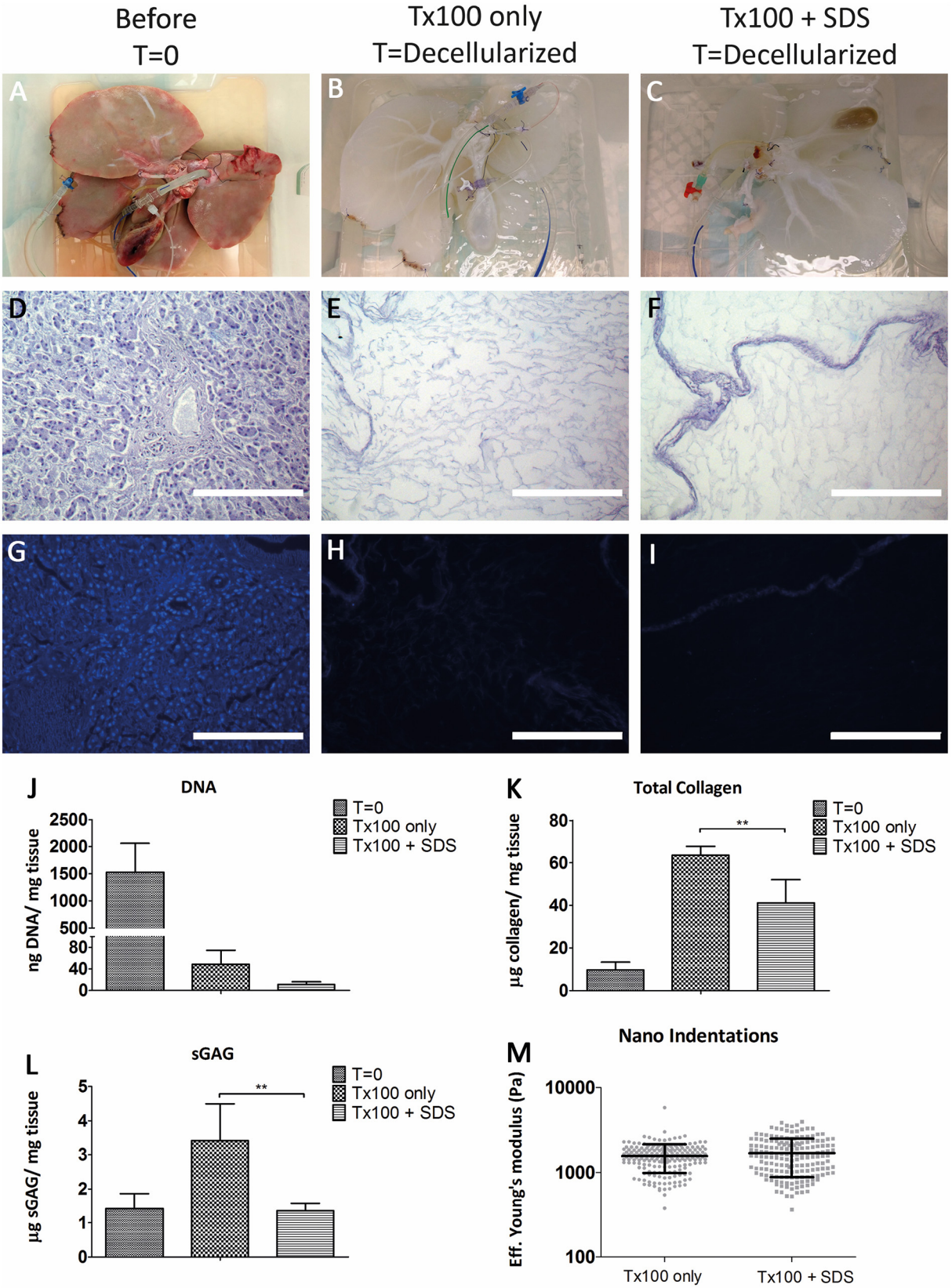

Fig. 2. Effective decellularization of porcine livers using oscillating pressure conditions. A: a porcine liver before decellularization. This image is representative of all six porcine livers that have been decellularized. B and C: porcine liver after decellularization with the Tx100 only protocol (B) and with the Tx100 + SDS protocol (C). D–F: HE stained paraffin sections of porcine livers before (D) and after decellularization (E and F). Scale bars represent 100 µm. G–I: DAPI stained paraffin sections of porcine livers before (G) and after decellularization (H and I). Scale bars represent 200 µm. J: the DNA content before and after decellularization. K: total collagen content before and after decellularization. L: sGAG content before and after decellularization. In J-L the mean + SD values (N = 3) are normalized against mg wet weight tissue (before) or ECM (after). ** $P < 0.01$, ANOVA. M: The effective Young's modulus of decellularized livers was measured by nano indentation. Tx100 only (N = 206 indentations) and Tx100 + SDS (N = 177 indentations). Results are shown as mean + SD. There are no significant difference between the two groups.

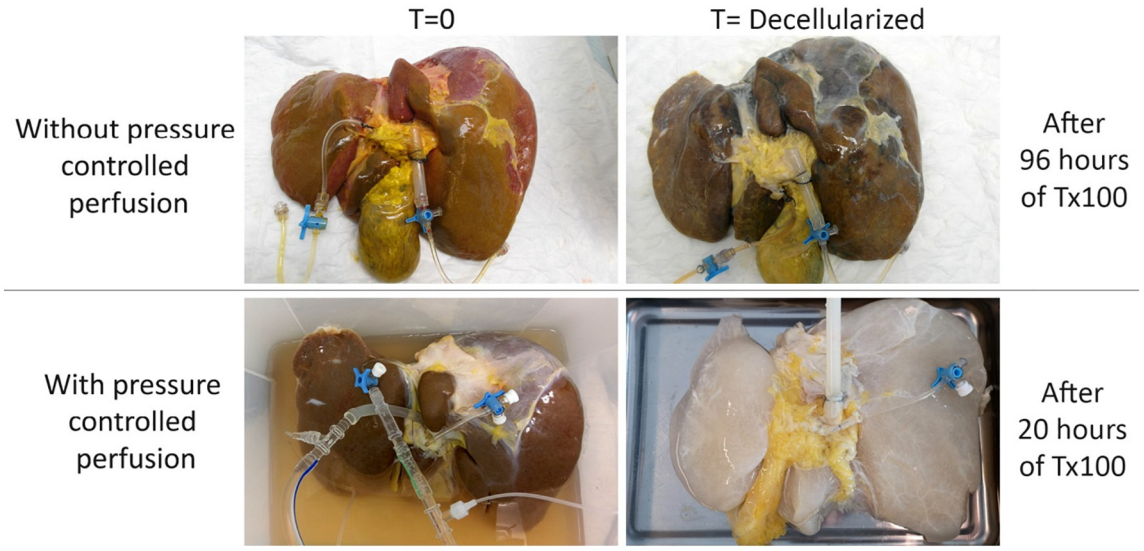

Fig. 3. Effective decellularization of human livers with pressure controlled perfusion using only Tx100. Shown is macroscopic overview of representative livers before and after decellularization. The top row shows a liver which was completely decellularized without pressure controlled perfusion following the previously published protocol. After 96 h of Tx100 perfusion the liver was completely decellularized, but did not lose its brown color. The bottom row shows a liver which was decellularized with pressure controlled perfusion. Shortly after starting perfusion with Tx100 the liver started losing its color. After 20 h of pressure controlled perfusion the liver was completely decellularized and had an off-white color. (For interpretation of the references to color in this figure legend, the reader is referred to the Web version of this article.)

nuclei were removed from the ECM, while the ECM architecture itself remained intact. CHP staining did not reveal further damage to the collagen fibers (Supplementary figure 1DEF).

Shortening protocol did not result in fully decellularized liver ECM, as residual cell remnants were seen in biopsies taken after completing 3 cycles (Supplementary Fig. 1B). Analysis of DNA content showed that DNA decreased from 1526 ng (SD: ± 487 ng)/mg wet weight tissue to 49 ng (SD: ± 21 ng)/mg wet weight tissue in the Tx100 only group and 11 ng (SD: ± 4 ng)/mg wet weight tissue in the Tx100 + SDS group (Fig. 2J). The difference between the two protocols was statistically not significant, but indicates that SDS might be more efficient in removing DNA from the ECM.

The total collagen content after decellularization (Fig. 2K) was significantly higher in the Tx100-only group (63.6 µg (SD: ± 3.4 µg) collagen/mg wet weight tissue) than in the Tx100 + SDS group (41.1 µg (SD: ± 8.9 µg) collagen/mg wet weight tissue; ($P < 0.01$). The total collagen content of the livers appears to increase three-fold after decellularization. This is caused by normalization of the collagen content to the 'mg wet weight tissue'. As the cells were removed from the tissue, the relative contribution of the remaining ECM compounds to the total wet weight of the sample increased. Therefore, direct comparisons between before and after decellularization could not be drawn. However, SDS had a significant negative impact on the collagen content of the decellularized ECM, as the total collagen content of the Tx100 + SDS group is lower than the Tx100 group.

Additionally, the sGAG content (Fig. 2L) of the decellularized livers differed significantly. The Tx100-only livers contained more sGAG (3.4 µg (SD: ± 0.9 µg) sGAG/mg wet weight tissue) than the Tx100 + SDS livers (1.4 µg (SD: ± 0.2 µg) sGAG/mg wet weight tissue); $P < 0.01$. When comparing this data to the T = 0 data, a similar trend was shown as with the collagen content. No direct comparison to the T = 0 sGAG content could be made due to the aforementioned shift in relative weight components to the total wet weight of the sample.

The lower total collagen and sGAG content in the Tx100 + SDS decellularized livers does not significantly affect the stiffness of the ECM after decellularization (Fig. 2M). The measured effective Young's modulus for the Tx100 group (1565Pa (SD: ± 575Pa)) was lower, but not significantly different than the measured effective Young's modulus of the Tx100 + SDS group (1687 Pa (SD: ± 805 Pa). The spread in the Tx100 + SDS group is slightly larger, because one of the livers had significant higher ($P < 0,001$) average effective Young's modulus (2271 Pa (SD: ± 776 Pa) compared to the other five livers (ranging from 1305 Pa to 1651 Pa). Between the other five livers (from both groups) no significant differences could be found.

Based on the previous findings, the Triton X-100-only protocol was chosen to establish a standardized clinical human whole-liver decellularization protocol.

3.2. Validation of the Tx100 only protocol on human livers

The human livers (n = 3) used in this study were declined for a variety of reasons, such as age of donor and/or long ischemia times. One liver was declined for transplantation due to a damaged hepatic artery. All three livers were 'donation after cardiac death' livers. The average age of donors was 49 years (SD: 24 years). The youngest donor was 15 years of age. The average body mass index of the donors was 25.3 (SD: 3.6) and the average weight of the livers ranged from 1.1 kg to 1.9 kg (average: 1.5 kg, SD: ± 0.25 kg).

Similar to porcine livers during the first half hour of Tx100 perfusion, small decellularized spots appeared near the surface of the livers (Supplementary Fig. 2A, Supplementary Video 2). During the first hour of Tx100 perfusion, the RPM of the pump drive was increased to an average of 150RPM (SD: 30RPM) in order to keep perfusion pressure constant at 120 mm Hg. After the first hour only minor adjustments (± 10 RPM) were required to maintain hepatic artery pressure at 120 mm Hg. Portal vein pressure ranged from 35 mm Hg to 60 mm Hg. Total perfusion time required was on average 30 h (20 h of perfusion with Tx100). After finishing the complete decellularization protocol with pressure controlled perfusion, the livers had a yellowish to white transparent color (Fig. 3 bottom right).

Supplementary video related to this article can be found at https://doi.org/10.1016/j.msec.2019.110200.

HE (Fig. 4B) and DAPI (Fig. 4D) stained paraffin sections showed that all cells and cellular debris was removed. Furthermore, these stained sections showed that the ECM remained intact. This was substantiated by SEM imaging (Fig. 4E and F), which also shows intact ECM. This was further supported by the CHP staining, which did not

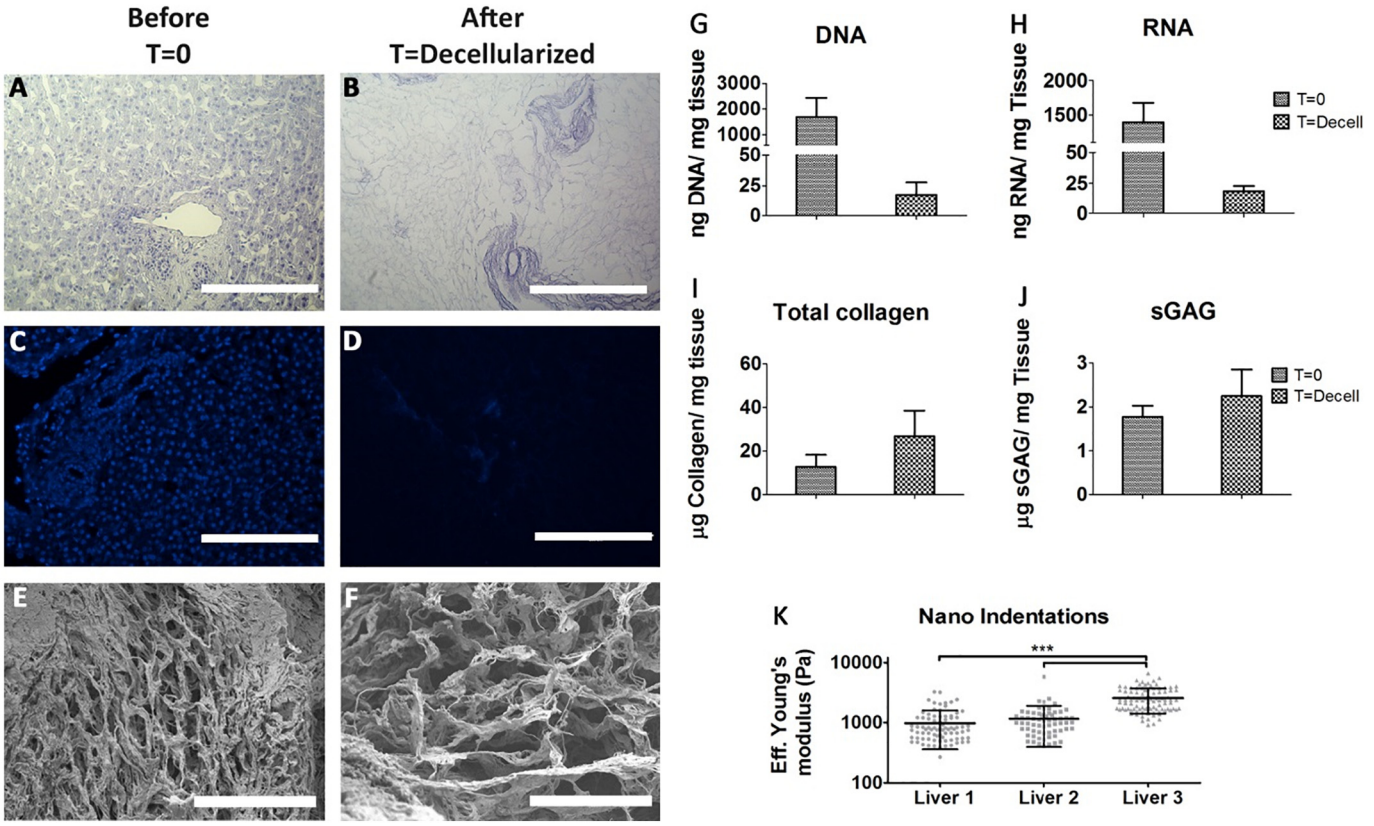

Fig. 4. Analysis of the ECM shows effective decellularization of human livers under oscillating pressure controlled perfusion. A–B: HE stained paraffin sections of human liver before (A) and after (B) decellularization. Scale bars represent 100 µm. C–D: DAPI stained paraffin sections of human liver before (C) and after (D) decellularization. Scale bars represent 200 µm. E–F: SEM images of decellularized liver ECM at 500x magnification (E) and 1000x magnification (F). Scale bars represent 100 µm (E) and 50 µm (F). DNA (G), RNA (H), Total collagen (I) and sGAG content (J) before and after decellularization for all three livers. Measured values are normalized against mg wet weight tissue (before) or ECM (after).K: Nano indentations from liver 1 (N = 81 indentations), Liver 2 (N = 65 indentations) and liver 3 (N = 97 indentations). 3*** P < 0,001, ANOVA Measured values are displayed as mean + SD.

reveal an increase in fluorescent signal as a response to damage collagen (Supplementary Figs. 1G and 1H). This indicates that the increased flow speeds, pressure and the oscillating flow conditions did not damage the ECM superstructure. The DNA yield after decellularization was 17.6 ng (SD: ± 8.4 ng)/mg wet weight tissue, which is a reduction of 99.0% (Fig. 4G). Furthermore, the remaining DNA did not consist of detectable double-stranded DNA, as no double-stranded DNA could be detected by the BioAnalyzer (Supplementary Fig. 2A). After complete decellularization, 18.4 ng (SD: ± 3.5 ng)/mg wet weight tissue of RNA was measured which was a 98.7% reduction (Fig. 4H). The BioAnalyzer did not detect any RNA peaks in the decellularization samples (Supplementary Fig. 2B).

3.3. Preservation of ECM molecules

After decellularization 25.4 µg (SD: +- 9.1 µg) collagen/mg wet weight tissue was measured (Fig. 4I). This is a two-fold increase compared to the non-decellularized samples (12.1 µg (SD: ± 4.2 µg) collagen/mg wet weight tissue). The average sGAG content (Fig. 4J) before decellularization was 1.7 µg (SD: ± 0.2 µg) sGAG/mg wet weight tissue and 2.2 µg (SD: ± 0.5 µg) sGAG/mg wet weight tissue after decellularization. The amounts of collagen and sGAG measured after decellularization were not similar to the amounts measured for the porcine liver decellularized with the Tx100-only protocol.

Significant differences regarding stiffness were found between the three livers using nano indentation measurements (Fig. 4K). Liver 1 is (979Pa (SD: ± 614 Pa)) and liver 2 (1154 Pa (SD: ± 753 Pa)) have lower effective Young's moduli than liver 3 (2560 Pa (SD: ± 1140 Pa)).

Furthermore, differences in fat content were seen between the three livers. All three livers had lipid droplets prior to decellularization (Fig. 5A, C and 5E). However, liver 2 contained lower amounts of fat droplets when compared to the other livers. This pattern was also seen after decellularization, where fat droplets remained within the decellularized ECM (Fig. 5B, D and 5F). This indicates that not all fat could be removed from the ECM using this protocol.

Lipofuscin, which is an age-related brown pigment that mainly consists of oxidized proteins and lipids [31], was found to be present in all human livers before decellularization, as determined by Sudan B Black staining (Fig. 5G, I and 5K). After decellularization almost all lipofuscin was successfully removed from the liver (Fig. 5H, J and 5L). With the previously published decellularization protocol, without pressure-controlled flow conditions, lipofuscin, was not removed from the ECM causing the decellularized livers to remain brown in color (Supplementary Fig. 3A, 3B and 3H) [20].

In addition the quantification of collagen content, collagens were also stained with PSR (Fig. 6A before decellularization, Fig. 6B after decellularization), which revealed that collagens remain present and that the ECM architecture remains intact. Furthermore, specific collagens were stained using specific antibodies against certain collagens. Collagen type I (Fig. 6C and 6D), type III (Fig. 6E and F) and type IV (Fig. 6G and H). All three types of collagen remain present after decellularization. The ECM architecture, of which collagens are an important part, appeared to have remained intact under the oscillating perfusion conditions.

3.4. Recellularization experiments

A two-dimensional recellularization experiment was performed by

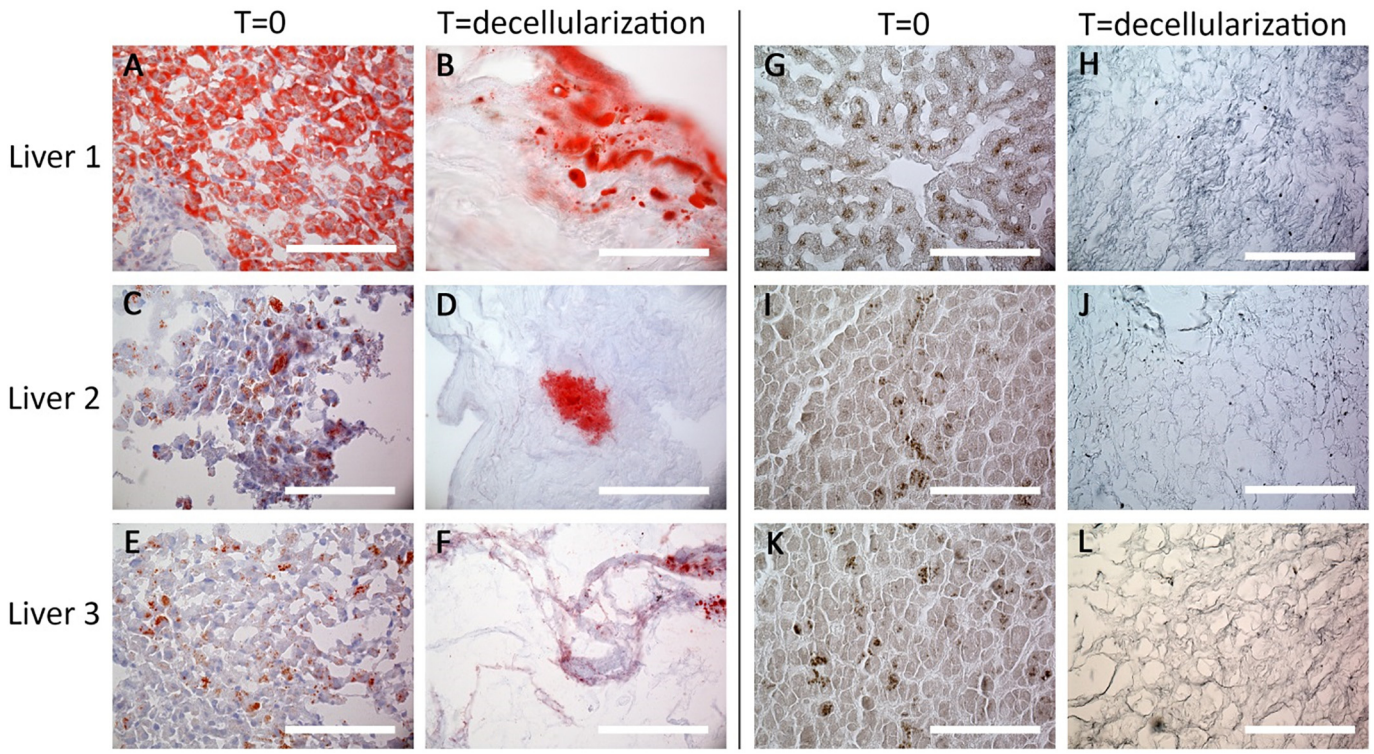

Fig. 5. Decellularization of human livers does not remove all lipids, but does remove lipofuscin. A–F: Oil red O stained cryosections of liver biopsies before (A, C and E) and after (B, D and E) decellularization. The red stained lipids are abundant in liver 1 (A), where small fat droplets are intracellular. Larger lipid droplets are seen in liver 2 (C) and 3 (E). Fat remains in the liver ECM after decellularization. G–H: Sudan B Black stained paraffin sections before (G, I and K) and after (H, J, L) decellularization. The lipofuscin present in the livers before decellularization is stained black and is granular in shape. Lipofuscin is removed from the ECM during the decellularization process, as almost no lipofuscin is stained after decellularization. All scale bars represent 100 μm. (For interpretation of the references to color in this figure legend, the reader is referred to the Web version of this article.)

seeding HEPG2 cells on to human decellularized ECM in order to determine whether all cytotoxic traces of detergent had been removed from the decellularized ECM. One day after addition of the HEPG2 to the circular discs, the cells started encapsulating the ECM. Histological evaluation was performed 21 days after seeding (Fig. 7A–C) and reveals that cells grew into the ECM (Fig. 7 A and B), however, the ECM was not fully populated with HEPG2. Additionally, the HEPG2 encapsulated the ECM completely, presenting a single layer of cells surrounding the ECM (Fig. 7C, black arrow). The cells did not show signs of abnormal necrosis or apoptosis (data not shown).

Cannulated decellularized porcine liver segments (Tx100 only) were used for more complex perfusion based recellularization experiments. Fig. 7D shows a cannulated segment of porcine liver ECM inside the humidified chamber of the isolated liver perfusion set up. The GFP-labelled HEPG2 cells were visible inside the arteries directly after infusion (Fig. 7E). Histological evaluation of the recellularized porcine ECM segments at day 11 revealed large areas of recellularized ECM with viable cells (Fig. 7F and G). HEPG2 cells were also found lining the walls of blood vessels (Fig. 7G).

4. Discussion

In this report we present a robust, effective and potentially clinically applicable method for human whole-liver decellularization to generate human liver scaffolds for bioengineering and transplantation. The major constraint in liver transplantation is shortage of donor organs. Thus, various tissue engineering approaches have been explored to find solutions to this problem. The main focus is to obtain acellular liver ECM that can be repopulated with normal liver cells in order to recreate a functional liver substitute. In 2004, a major step was taken by the group of Lin [32] who showed successful decellularization of a porcine liver. Repopulation of this scaffold with primary rat hepatocytes resulted in higher albumin and urea synthesis when compared to monolayers of the primary hepatocytes cultured on collagen gels, indicating greater functional potential of cells cultured in a 3D ECM scaffold. More recently, Baptista confirmed the repopulation of decellularized porcine liver with human hepatocyte progenitor cells for up to 13 days [2]. The availability of porcine livers, comparable to human size livers, make porcine livers an interesting source of decellularized ECM for tissue engineering purposes [1,3,24].

However, the ultrastructure of porcine liver differs significantly from that of human liver. Porcine liver has well defined lobules outlined by connective tissue, which is absent in healthy human liver but present in fibrotic liver [33]. Therefore, it may not represent the ideal ECM for human liver tissue engineering. The presence of connective tissue in porcine livers could also explain why human liver 1 and human liver 2 have lower effective Young's moduli than the porcine livers (both groups). Only human liver 3 had a higher Young's modulus than the porcine livers, which could indicate that this liver was (slightly) fibrotic.

Given the wide availability of human donor livers, deemed unsuitable for liver transplantation, optimal use of these organs for regenerative medicine purposes can be pursued. As previously shown, human livers can be decellularized, however, detergent perfusion times ranged from a couple of days to weeks [20,28]. To facilitate larger scale clinical application, a more efficient standard whole-organ liver decellularization protocol is required, which would be applicable to all human research livers. Recently, Struecker showed that oscillating pressure conditions increased decellularization efficiency in porcine livers with significantly reduced decellularization times [25].

In this study, we successfully optimized our previously reported method for the decellularization of whole-organ human livers by

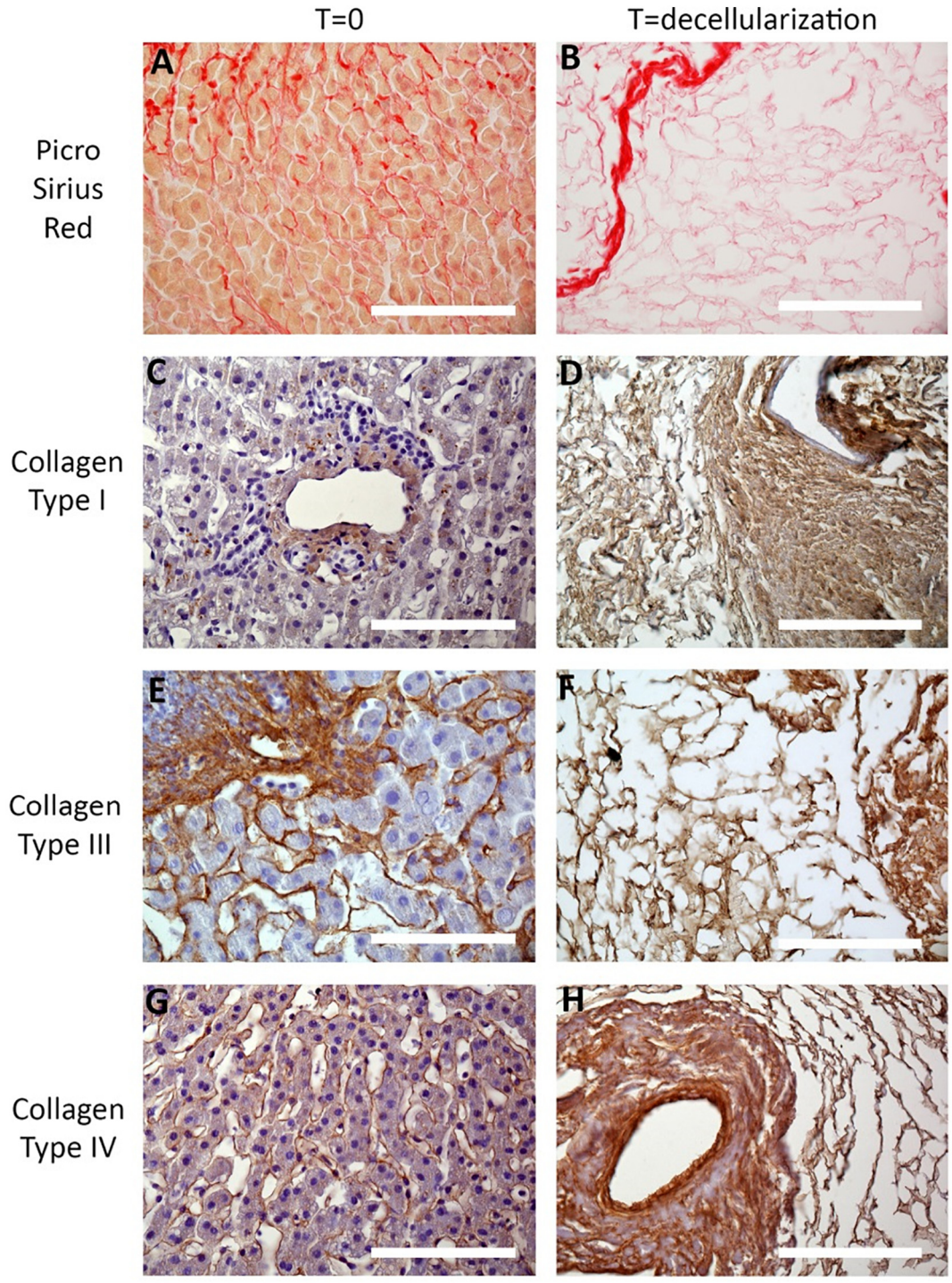

Fig. 6. Preservation of important Collagen proteins after decellularization of human livers with pressure controlled perfusion. A, B: PSR stained paraffin section before (A) and after (B) decellularization. C, D: Collagen type 1 before (C) and after (D) decellularization. E, F: Collagen type III before (E) and after (F) decellularization. G, H: Collagen type IV before (G) and after (H) decellularization. Scale bars represent 100 μm.

maintaining constant pressures on the hepatic artery by adding pressure-controlled machine perfusion. This seemed to make the decellularization process more robust and standardized, as the aforementioned differences in duration of detergent perfusion were not encountered. The time during which the organ is exposed to Tx100 was decreased from 62-94 h–20 h. Total time required for perfusing the liver with pressure-controlled perfusion was on average 32 h (not including a 10–14 day period of storage at 4 °C). By decreasing the time required for decellularizing the whole organ, the exposure time of detergents to ECM, which can potentially damage or remove ECM components, was also significantly decreased.

To further minimize the damage to the ECM, we used a protocol without SDS, as this was shown to remove or denature ECM components during decellularization of tissues, such as porcine urinary bladder tissue [1,29]. Reports on liver decellularization, using both Tx100 and SDS as detergents, show that sGAG levels are similar to the before decellularization samples [25]. This finding is confirmed by our decellularization experiments on porcine liver with Tx100 and SDS. The Tx100-only decellularized porcine livers contain 2.5 times more sGAG than the Tx100 + SDS decellularized livers. We hypothesize that no

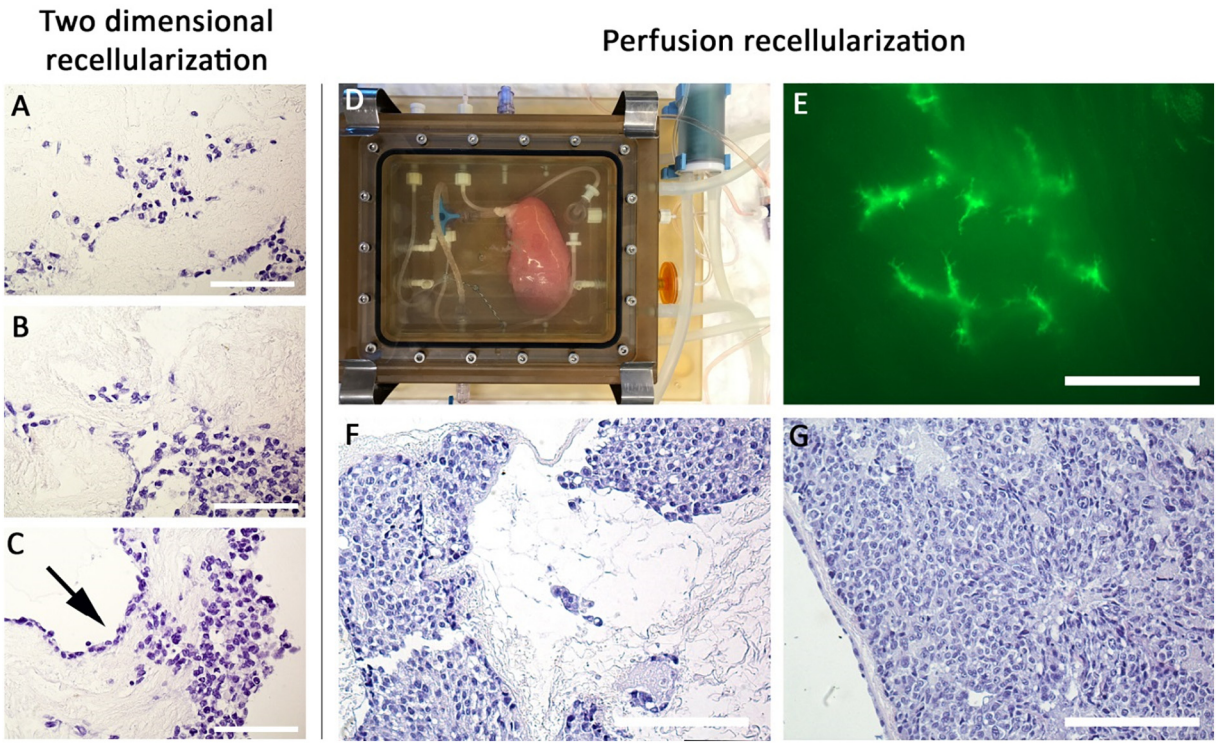

Fig. 7. Decellularized liver ECM can be used as a scaffold for tissue engineering purposes. A–C: HEPG2 cells invading the 200 μm thick section of human ECM. The cells can be found inside the ECM (A and B). HEPG2 encapsulated the ECM, surrounding the ECM with a single cell layer (black arrow in C). Scale bars (ABC) represent 100 μm. D: Perfusion-based recellularization of porcine liver ECM with HEPG2 cells was performed using a humidified chamber of the isolated liver perfusion set up. The decellularized porcine liver segment is connected to the perfusion setup via a three-way stop cock. E: the GFP signal of the infused HEPG2 cells can be seen inside the branching arteries of the porcine liver segment. Scale bar represents 2000 μm. F and G show HE stained paraffin slides of recellularized ECM after 11 days. HEPG2 partially repopulate the parenchymal ECM. Scale bars represent 100 μm.

comparison can be made between the 'before tissue' and the 'decellularized ECM' due to a shift in the relative weight component of the ECM to the weight of the sample. This makes it difficult to determine whether sGAG have been removed from the ECM during the decellularization procedures. However, the data does show that the Tx100-only protocol retains more sGAG than the Tx100 + SDS protocol.

This also holds true for the total collagen content. The Tx100-only protocol retains 1.5 times more collagen than the porcine liver decellularized with Tx100 + SDS protocol. Both the sGAG and total collagen content data confirms that SDS has a deleterious effect on these ECM components. Interestingly, the use of SDS did not affect to the effective Young's modulus of a nanoscale.

The aforementioned ECM components play essential roles in various biological processes and are therefore also important to maintain for downstream applications of the decellularized ECM, such as liver tissue engineering purposes [3,17,18]. Therefore, the Tx100-only porcine liver decellularization protocol was translated towards a protocol for whole-organ human livers.

Similar to the porcine liver, decellularization of the human livers with only Tx100 and pressure conditions, yielded completely decellularized human livers. Interestingly, the Tx100-only pressure-controlled perfusion protocol was capable of clearing lipofuscin from the ECM while lipofuscin could not be removed using the previously published protocol without pressure controlled perfusion (Figs. 3 and Fig. 5H,J,L and Supplementary Fig. 3F) [20]. Despite this clearance of lipofuscin, our method was not yet able to completely remove lipid droplets and/or fat from the ECM. This may be important for future application of the scaffolds, as it is likely that due to high-fat diets and increasing obesity, discarded livers will contain more fat in the near future [34]. The implication of remaining fat droplets for recellularization is not yet clear, but considering fatty liver disease and steatohepatitis, further focus on the total removal of lipids seems warranted. Additional perfusion steps with polar solvents could be helpful to totally remove fat from the ECM [35,36].

Other issues that are important in the future application of liver scaffolds for transplantation purposes are the removal of the Tx100 detergent residues and the sterility of the scaffold. Current definitions of decellularized ECM focus solely on microscopically visible cells remnants or the presence of detectable double-stranded DNA [1]. However, for clinical applications more stringent forms of quality control are required, which include screening for the presence of residual detergents after decellularization and screening for microbial/fungal infections [37,38]. Currently, detergent residues are tested with cyto-toxicity assays [39,40]. To further prove that detergents have been removed completely from the ECM, colorimetric assay (for SDS) [41] or time of flight secondary ion mass spectroscopy [42] could be an alternative to cyto-toxicity assay. Detection of Tx100 has also been described for chemiluminescent [43] or UV spectroscopy methods [44], but these techniques have not yet been tested on decellularized ECM. For clinical applications a simple, cheap and accurate Tx100 detection method would be ideal.

The two-dimensional recellularization experiments with HEPG2 cells lasted over 21 days and results showed viable cells inside the human ECM. This data confirms removal of detergents below cytotoxic levels. Although, decellularization of the livers is performed in a non-sterile lab environment, no bacterial infections were encountered during recellularization of the ECM with HEPG2 cells. However, for future applications the decellularization setup can be easily adapted towards a closed-loop system in a closed and sterile environment for more stringent control.

The recellularization experiments as presented here, have been carried out using a HEPG2 cell line, which is derived from a well differentiated hepatocellular carcinoma [45]. Although this cell line has *in vitro* applications, it is unsuitable for *in vivo* applications due to its

cancerous. For (personalized) tissue engineering applications, adult stem cells, such as bi-potent liver derived organoids [46] or induced pluripotent stem cells could be a good cell source in the near future [3].

These decellularization protocols provide an effective way to produce decellularized liver ECM from both porcine and human sources in a standard manner. The liver ECM has great potential to be used as a scaffold for tissue engineering or regenerative medicine purposes. The next step is to further develop the perfusion-based recellularization in order to achieve complete repopulation of the liver parenchyma, the vasculature network and biliary tree. Ideally, the (patient's own) liver derived organoids could be used to create functional hepatic constructs for transplantation purposes.

5. Conclusion

The decellularization protocols with pressure controlled perfusion are effective in decellularizing both porcine and human livers, as these protocols yielded completely decellularized livers, which were white in color and semi-transparent. The addition of pressure-controlled perfusion did decrease the time required to fully decellularize livers considerably, but did not remove ECM components or damage the ultrastructure of the ECM.

Acknowledgements

The isolated liver perfusion system from Harvard Apparatus was purchased with funding from the 'Maurits en Anna de Kock' foundation (2018).

Abbreviations

ANOVA	Analysis of variance
CHP	Collagen Hybridizing Peptide
DAPI	4′,6-diamidino-2-phenylindole
dH_2O	demineralized water
ECM	Extra cellular matrix
HE	hematoxylin-Eosin
HMDS	Hexamethyldisilazane
IBP	Invasive blood pressure
IHC	Immunohistochemistry
NTS	Dutch transplant foundation
PFA	Paraformaldehyde
PSR	Picrosirius Red
RPM	Rounds per minute
RT	Room Temperature
SD	Standard deviation
SDS	Sodium dodecyl sulfate
sGAG	sulfated Glycosaminoglycan
Tx100	Triton-x-100

Appendix A. Supplementary data

Supplementary data to this article can be found online at https://doi.org/10.1016/j.msec.2019.110200.

References

[1] P.M. Crapo, T.W. Gilbert, S.F. Badylak, An overview of tissue and whole organ decellularization processes, Biomaterials 32 (12) (2011) 3233–3243.
[2] P.M. Baptista, et al., The use of whole organ decellularization for the generation of a vascularized liver organoid, Hepatology 53 (2) (2011) 604–617.
[3] J. Willemse, et al., From organoids to organs: bioengineering liver grafts from hepatic stem cells and matrix, Best Pract. Res. Clin. Gastroenterol. 31 (2) (2017) 151–159.
[4] M. Blachier, et al., The burden of liver disease in Europe: a review of available epidemiological data, J. Hepatol. 58 (3) (2013) 593–608.
[5] Eurotransplant, Annual Report 2017, Eurotransplant international foundation, 2018.
[6] W.R. Kim, et al., Hyponatremia and mortality among patients on the liver-transplant waiting list, N. Engl. J. Med. 359 (10) (2008) 1018–1026.
[7] L.G. Griffith, G. Naughton, Tissue engineering–current challenges and expanding opportunities, Science 295 (5557) (2002) 1009–1014.
[8] R. Lanza, R. Langer, J.P. Vacanti, Principles of Tissue Engineering, Academic press, 2011.
[9] J.P. Vacanti, R. Langer, Tissue engineering: the design and fabrication of living replacement devices for surgical reconstruction and transplantation, Lancet 354 (1999) S32–S34.
[10] J.S. Lee, et al., Liver extracellular matrix providing dual functions of two-dimensional substrate coating and three-dimensional injectable hydrogel platform for liver tissue engineering, Biomacromolecules 15 (1) (2014) 206–218.
[11] M.J. Gomez-Lechon, et al., Competency of different cell models to predict human hepatotoxic drugs, Expert Opin. Drug Metabol. Toxicol. 10 (11) (2014) 1553–1568.
[12] G. Agmon, K.L. Christman, Controlling stem cell behavior with decellularized extracellular matrix scaffolds, Curr. Opin. Solid State Mater. Sci. 20 (4) (2016) 193–201.
[13] K.-M. Park, et al., Decellularized liver extracellular matrix as promising tools for transplantable bioengineered liver promotes hepatic lineage commitments of induced pluripotent stem cells, Tissue Eng. A 22 (5–6) (2016) 449–460.
[14] E. Arriazu, et al., Extracellular matrix and liver disease, Antioxidants Redox Signal. 21 (7) (2014) 1078–1097.
[15] O. Barakat, et al., Use of decellularized porcine liver for engineering humanized liver organ, J. Surg. Res. 173 (1) (2012) e11–e25.
[16] B.E. Uygun, et al., Organ reengineering through development of a transplantable recellularized liver graft using decellularized liver matrix, Nat. Med. 16 (7) (2010) 814–820.
[17] M. Klaas, et al., The alterations in the extracellular matrix composition guide the repair of damaged liver tissue, Sci. Rep. 6 (2016) 27398.
[18] B.P. Chan, K.W. Leong, Scaffolding in tissue engineering: general approaches and tissue-specific considerations, Eur. Spine J. 17 (4) (2008) 467–479.
[19] M. Rojkind, M.A. Giambrone, L. Biempica, Collagen types in normal and cirrhotic liver, Gastroenterology 76 (4) (1979) 710–719.
[20] M.M.A. Verstegen, et al., Decellularization of whole human liver grafts using controlled perfusion for transplantable organ bioscaffolds, Stem Cells Dev. 26 (18) (2017) 1304–1315.
[21] J. De Kock, et al., Simple and quick method for whole-liver decellularization: a novel in vitro three-dimensional bioengineering tool? Arch. Toxicol. 85 (6) (2011) 607–612.
[22] T. Shupe, et al., Method for the decellularization of intact rat liver, Organogenesis 6 (2) (2010) 134–136.
[23] K. Hillebrandt, et al., Procedure for decellularization of rat livers in an oscillating-pressure perfusion device, J. Vis. Exp. : J. Vis. Exp. (102) (2015) e53029-e53029.
[24] N.E. Buhler, et al., Controlled processing of a full-sized porcine liver to a decellularized matrix in 24 h, J. Biosci. Bioeng. 119 (5) (2015) 609–613.
[25] H.K. Struecker B, R. Voitl, A. Butter, R.B. Schmuck, A. Reutzel-Selke, D. Geisel, K. Joehrens, P.A. Pickerodt, N. Raschzok, G. Puhl, P. Neuhaus, J. Pratschke, I.M. Sauer, Porcine liver decellularization under oscillating pressure conditions: a technical refinement to improve the homogeneity of the decellularization process, Tissue Eng. C Methods 21 (3) (2014) 303–313.
[26] J. Bao, et al., Hemocompatibility improvement of perfusion-decellularized clinical-scale liver scaffold through heparin immobilization, Sci. Rep. 5 (2015) 10756.
[27] Q. Wu, et al., Optimizing perfusion-decellularization methods of porcine livers for clinical-scale whole-organ bioengineering, BioMed Res. Int. 2015 (2015) 785474-785474.
[28] G. Mazza, et al., Decellularized human liver as a natural 3D-scaffold for liver bioengineering and transplantation, Sci. Rep. 5 (2015) 13079.
[29] D.M. Faulk, et al., The effect of detergents on the basement membrane complex of a biologic scaffold material, Acta Biomater. 10 (1) (2014) 183–193.
[30] N.P. van Til, et al., Lentiviral gene therapy of murine hematopoietic stem cells ameliorates the Pompe disease phenotype, Blood 115 (26) (2010) 5329–5337.
[31] U.T. Brunk, A. Terman, Lipofuscin: mechanisms of age-related accumulation and influence on cell function, Free Radic. Biol. Med. 33 (5) (2002) 611–619.
[32] P. Lin, et al., Assessing porcine liver-derived biomatrix for hepatic tissue engineering, Tissue Eng. 10 (7–8) (2004) 1046–1053.
[33] Z.D. Goodman, Grading and staging systems for inflammation and fibrosis in chronic liver diseases, J. Hepatol. 47 (4) (2007) 598–607.
[34] Z.M. Younossi, et al., Global epidemiology of nonalcoholic fatty liver disease—meta-analytic assessment of prevalence, incidence, and outcomes, Hepatology 64 (1) (2016) 73–84.
[35] L.W. Dunne, et al., Human decellularized adipose tissue scaffold as a model for breast cancer cell growth and drug treatments, Biomaterials 35 (18) (2014) 4940–4949.
[36] L.E. Flynn, The use of decellularized adipose tissue to provide an inductive microenvironment for the adipogenic differentiation of human adipose-derived stem cells, Biomaterials 31 (17) (2010) 4715–4724.
[37] D.J. Rosario, et al., Decellularization and sterilization of porcine urinary bladder matrix for tissue engineering in the lower urinary tract, Regen. Med. 3 (2) (2008) 145–156.
[38] J.J. Uriarte, et al., Mechanical properties of acellular mouse lungs after sterilization by gamma irradiation, J. Mech. Behav. Biomed. Mater. 40 (2014) 168–177.
[39] S. Cebotari, et al., Detergent decellularization of heart valves for tissue engineering: toxicological effects of residual detergents on human endothelial cells, Artif. Organs 34 (3) (2010) 206–210.
[40] Y. Wang, et al., Method for perfusion decellularization of porcine whole liver and kidney for use as a scaffold for clinical-scale bioengineering engrafts,

Xenotransplantation 22 (1) (2015) 48–61.
[41] B. Zvarova, et al., Residual detergent detection method for nondestructive cytocompatibility evaluation of decellularized whole lung scaffolds, Tissue Eng. C Methods 22 (5) (2016) 418–428.
[42] L.J. White, et al., The impact of detergents on the tissue decellularization process: a ToF-SIMS study, Acta Biomater. 50 (2017) 207–219.
[43] X. Liu, et al., Chemiluminescence determination of surfactant Triton X-100 in environmental water with luminol-hydrogen peroxide system, Chem. Cent. J. 3 (2009) 7-7.
[44] B. Pavlovic, et al., Direct UV spectrophotometry and HPLC determination of triton X-100 in split virus influenza vaccine, J. AOAC Int. 99 (2) (2016) 396–400.
[45] S. Wilkening, F. Stahl, A. Bader, Comparison of primary human hepatocytes and hepatoma cell line HEPG2 with regard to their biotransformation properties, Drug Metab. Dispos. 31 (8) (2003) 1035–1042.
[46] M. Huch, et al., Long-term culture of genome-stable bipotent stem cells from adult human liver, Cell 160 (1–2) (2015) 299–312.